



An Exact Algorithm for the Linear Tape Scheduling Problem

Valentin Honoré, Bertrand Simon, Frédéric Suter

► To cite this version:

Valentin Honoré, Bertrand Simon, Frédéric Suter. An Exact Algorithm for the Linear Tape Scheduling Problem. 2021. hal-03482022v1

HAL Id: hal-03482022

<https://cnrs.hal.science/hal-03482022v1>

Preprint submitted on 16 Dec 2021 (v1), last revised 4 May 2022 (v3)

HAL is a multi-disciplinary open access archive for the deposit and dissemination of scientific research documents, whether they are published or not. The documents may come from teaching and research institutions in France or abroad, or from public or private research centers.

L'archive ouverte pluridisciplinaire **HAL**, est destinée au dépôt et à la diffusion de documents scientifiques de niveau recherche, publiés ou non, émanant des établissements d'enseignement et de recherche français ou étrangers, des laboratoires publics ou privés.

An Exact Algorithm for the Linear Tape Scheduling Problem

Valentin Honoré, Bertrand Simon, Frédéric Suter

IN2P3 Computing Center / CNRS, Lyon - Villeurbanne, France
valentin.honore@cc.in2p3.fr, bertrand.simon@cc.in2p3.fr, frederic.suter@cc.in2p3.fr

Abstract

Magnetic tapes are often considered as an outdated storage technology, yet they are still used to store huge amounts of data. Their main interests are a large capacity and a low price per gigabyte, which come at the cost of a much larger file access time than on disks. With tapes, finding the right ordering of multiple file accesses is thus key to performance. Moving the reading head back and forth along a kilometer long tape has a non-negligible cost and unnecessary movements thus have to be avoided. However, the optimization of tape request ordering has then rarely been studied in the scheduling literature, much less than I/O scheduling on disks. For instance, minimizing the average service time for several read requests on a linear tape remains an open question.

Therefore, in this paper, we aim at improving the quality of service experienced by users of tape storage systems, and not only the peak performance of such systems. To this end, we propose a reasonable polynomial-time exact algorithm while this problem and simpler variants have been conjectured NP-hard. We also refine the proposed model by considering U-turn penalty costs accounting for inherent mechanical accelerations. Then, we propose a low-cost variant of our optimal algorithm by restricting the solution space, yet still yielding an accurate suboptimal solution. Finally, we compare our algorithms to existing solutions from the literature on logs of the mass storage management system of a major datacenter. This allows us to assess the quality of previous solutions and the improvement achieved by our low-cost algorithm. Aiming for reproducibility, we make available the complete implementation of the algorithms used in our evaluation, alongside the dataset of tape requests that is, to the best of our knowledge, the first of its kind to be publicly released.

1 Introduction

Initially designed for media recording, the usage domain of magnetic tapes has broadened over the decades and remains a real competitor to disk storage even for scientific data. The main advantages of this storage medium are a large storage capacity for a reasonable price, a better data preservation, better security, and better energy efficiency. Indeed, it has been estimated that total costs are reduced by an average factor of 6 when archiving data on tape rather than disks [21].

Recent tape cartridges can store up to 10 terabytes of data on a one-kilometer-long physical storage, longitudinally divided into few bands which are each also longitudinally divided into dozens of wraps. Wraps are in turn divided into dozens of tracks. All tracks in a given wrap are read or written simultaneously. A tape is then composed of hundreds of parallel wraps which are logically linked together in a *linear serpentine*. Intuitively, the storage space can be seen as a single linear wrap coiled like a serpent on the tape.

Thousands of such cartridges are usually stored on the shelves of robotic libraries, as books would be stored in an actual library. Then, when data on a given cartridge is not needed, its storage does not induce any power consumption, and it cannot be accessed by intruders. All these advantages of tape storage made it an unavoidable candidate for the storage of the exabytes of data produced at CERN by the Large Hadron Collider experiments [10] or data related to European weather forecast [20].

The huge amount of data stored in such tape libraries, typically hundreds of petabytes, is usually managed by a Mass Storage Management System (*e.g.*, IBM HPSS or HPE DMF) which keeps track of the exact location of the files stored on tapes and answers to users' requests. When a particular file is needed, the tape it is on will be fetched by a robotic arm, brought to a tape drive, and loaded. Then, the reading head of the tape drive is positioned to the beginning of the file to read, or to the first available space to write new data, and the I/O operation eventually occurs.

The main drawback of tape storage is the high latency to access a given file. Mounting a tape into a tape reader requires a delay of about a minute [5]. Moreover, seeking from one file to another adds more delay to place the reading head on the correct wrap and adapt the longitudinal position of the tape in front of the head. When accesses to multiple files are requested, finding the right ordering of these accesses is thus key to performance. Moving the reading head back and forth along a kilometer long tape has a non-negligible cost and unnecessary movements thus have to be avoided. However, the optimization of tape request ordering has then rarely been studied in the scheduling literature, much less than I/O scheduling on disks. For instance, minimizing the average service time for several read requests, *i.e.*, the average time at which each request is read, on a linear tape remains an open question.

Therefore, in this paper, we aim at improving the quality of service experienced by users of tape storage systems, and not only the peak performance of such systems. To this end, we consider a simplified model of magnetic tape composed of a single linear track. This is a strong assumption as the serpentine nature of tapes leads to important optimization decisions. However, it still reflects local batch requests which would target files belonging to the same wrap. We also believe it is a fundamental model which should be deeply understood. In this model, a tape can therefore be seen as a linear sequence of files which all have to be read from the left to the right. The input of the problem we consider is a list of files that are requested, associated with a number of requests for each file. The objective is to design a schedule (*i.e.*, a trajectory of the reading head on the linear tape) to read all the requested files when the reading head is initially positioned on the right of the tape. We consider the average service time as a metric, to ensure a fair service among all requests. In order to model the temporality of a given schedule, we assume that the speed of the tape is constant, although it is a mechanical device with inertia. We moderate this inaccuracy by taking into account the deceleration induced by a U-turn of the tape as a nominal penalty. Note that we do not consider write requests, which are usually done separately, nor update requests, which are avoided as they damage nearby data. Following [6], we refer to this problem as the Linear Tape Scheduling Problem (LTSP), noting that our model differs from theirs by accounting for U-turn penalties.

LTSP has been previously studied by Cardonha and Real [6, 7] and conjectured to be impossible to be solved efficiently. Indeed, even simpler variations restricting either file requests to be unique or file sizes to be equal have been conjectured NP-hard [7]. We answer this open question in this paper by providing a polynomial algorithm optimally solving the unrestricted LTSP problem, also considering U-turn penalties. More precisely, we show that a carefully designed Dynamic Programming implementation (technique which has been considered in [7] but was deemed not conclusive) allows us to compute an optimal schedule in a reasonable polynomial time. We then provide a faster suboptimal algorithm and compare the performance of these two original algorithms to that of existing algorithms on a dataset built from the recent history of the tape library of the IN2P3 Computing Center.

The remainder of this paper is organized as follows. In Section 2, we review the literature on tape scheduling and related optimization problems. In Section 3, we define and discuss precisely the model and the objective function. In Section 4 we expose our algorithmic solutions to this problem. Finally, in Section 5, we present the results of our simulations on a real-world dataset.

2 Related work

The closest works to the present paper [6, 7] study LTSP under the same tape model, except for the U-turn penalties which are not considered. The authors note that the algorithm minimizing the maximal service time, *i.e.*, the time at which all files are read, can present an average service time arbitrarily far from the optimal. They show that the opposite algorithm reading the rightmost files first is however a 3-approximation, and

design a few greedy optimizations. Finally, they provide several heuristics for the online variant and compare their solutions on simulations.

LTSP is related to several well-studied problems in theoretical computer science. The most famous one is probably the Traveling Salesperson Problem, where the goal is to visit n points as fast as possible following given travel times between each pair of points. This problem is notoriously NP-hard in general metrics [16] so approximation algorithms and special cases have been studied extensively. One of the most recent development has been the design of an algorithm surpassing the long-standing approximation ratio of 1.5 [15]. LTSP is closer to its restriction on the real line, for which it can be solved in $O(n^2)$ [3].

A key difference between LTSP and the Traveling Salesperson Problem resides in the objective function, as LTSP aims at minimizing the average service time. This objective is captured by the Minimum Latency Problem (also called Traveling Repairperson Problem) for which the best known approximation ratio is 3.59 [8]. This problem is already strongly NP-hard on trees [24], although it admits a PTAS [25], but can be solved polynomially on the line if there are no deadlines [1].

Keeping the average service time objective function but adding delays at every visited vertex leads to a more general definition of the Traveling Repairperson Problem. This problem is strongly NP-hard on the line when deadlines or release times are involved [4] but its complexity when requests can be served at any time is still unknown.

A different kind of related problems has been studied under the name of Dial-A-Ride. Here, requests are composed of a source and a destination and the goal is to move vehicles to transport all requests from their source to their destination. Several variants of the problem exist, even restricted to the offline setting, depending on the presence of release times or the number and capacities of the vehicles, see [11]. The Dial-A-Ride problem can be seen as a generalization of LTSP but is often studied with the objective of minimizing the total service time. A simpler variant, close to our problem, considers a single vehicle able to transport one request at a time without being able to drop it before the destination, and is shown to be polynomially solvable [2] when minimizing the total service time. A formulation aiming at minimizing the average service time has been shown to be NP-hard, relying on request irregularities (overlapping trips in different directions) [11, Theorem 7] which cannot happen in LTSP where requests are unidirectional and files are disjoint.

We did not cover all the work done on the online version of these problems, when future requests are unknown, but we refer the reader to [3] for an overview of such results.

The literature on tape scheduling is rather scarce although the role of tape libraries is far from negligible in modern computing centers. Contrarily to this paper, most studies consider a more complex tape geometry, usually a serpentine. Hillyer and Silberschatz [13] focus on low-level hardware information (*key points*) to evaluate several heuristics. Sandsta and Midtstraum [22] propose a low-cost function to approximate the seeking time between two points of the tape. More and Choudhary [19] design algorithms to schedule the mounts of different tapes in a library. Melia [18] evaluates the seek times between any two points of a recent tape, data which is used as input in a few heuristics to compare their performance. Software designed to optimize tape usage appear to often sort read requests based on their tape position [23, 26]. A common point to these studies is that the focus has mostly been on cost modeling due to the two-dimensional nature of the tape and low-level hardware aspects, but publicly released scheduling algorithms are often greedy ones. A proprietary solution used by some tape libraries, named Recommended Access Order (RAO), exploits such two-dimensional tape information but its underlying algorithm is not available [14, Section 4.27].

3 Model and Problem Descriptions

We consider a linear tape of length m , divided successively in n_f disjoint files (f_1, \dots, f_{n_f}) of integer size $s(f_i)$. Let $\ell(f_i)$ be the *length* between the left of the tape and the left of the file f_i and $r(f_i) = \ell(f_i) + s(f_i)$. We say that $f_i < f_j$ if file f_i is located on the left of f_j , i.e., $\ell(f_i) < \ell(f_j)$. We are given a set of n requests on n_{req} files among the n_f files of the tape, with possible duplicates, where each request is a file. Let $x(f_i)$ be the number of requests allocated to file f_i .

At the beginning, the reading head is positioned on the right of the tape. A request is fulfilled when its file has been traversed from the left to the right by the reading head. We assume the reading head moves at constant

speed (the tape is actually moving and the head is fixed, but switching roles helps the exposure), a time unit being necessary to traverse a file chunk of size 1 in either direction. We also consider a time penalty U for each U-turn performed by the head.

The main limitation of this model concerns the track geometry. Modern tapes are not constituted of a single linear track, and being aware of their serpentine geometry is essential to optimize the reading sequence and seeking costs. However, this simpler model is able to emulate accurately local considerations when files written in the same period are located in a single track. It is also fundamental to deeply understand the complexity of such a model knowing that the serpentine model is much closely related to NP-hard problems such as the Traveling Salesperson Problem.

The assumption of the tape moving at a constant speed in front of the reading head is obviously inaccurate due to acceleration and deceleration inherent to mechanical devices. However, the cruise speed is typically reached fast so this approximation is satisfactory apart from U-turns. The nominal U-turn penalty used to take into account these slow-downs therefore improves the model accuracy.

Other limitations of the model such as the undifferentiated reading speed or the forced starting position of the head are discussed as extensions in the conclusion.

The objective is to provide a *schedule*, *i.e.*, a trajectory of the reading head on the tape, that serves all requests and minimizes the sum of service times of requests, *i.e.*, the sum of the times needed before each request is satisfied. Note that we formally define the objective as minimizing the sum, but it is more intuitive in terms of a quality of service to speak about the average service time, an objective which is completely equivalent.

A simple lower bound *VirtualLB* on the optimal solution is achieved by using n virtual heads serving each request optimally, *i.e.*, each reading head moves directly to the left of its assigned file then reads it.

$$VirtualLB = \sum_f x(f) \cdot (m - \ell(f) + s(f) + U).$$

Minimizing the average service time is one of the most classic scheduling objective functions with the maximal service time. The latter has been the main focus of studies on the serpentine model as it minimizes the time spent using the tape which decreases wear and delay of other tapes reads. However, in the linear tape model, minimizing the maximal service time is trivial while minimizing the average service time leads to more fairness among users. This is especially true in a case of low tape usage in which tapes are rarely waiting to be mounted.

4 Algorithm

This section presents the main contribution of this paper, the **DP** algorithm solving LTSP in time $O(n_{req}^3 \cdot n)$. Before describing **DP**, we start with giving useful definitions, preliminary remarks, and brief descriptions of existing solutions. We then also present the **LOGDP** variant algorithm, which limits the search space of **DP** to provide a suboptimal solution with a smaller time complexity of $O(n_{req} \cdot n \cdot \log^2 n_{req})$.

4.1 Preliminaries

In this section, we study the structure of optimal solutions to provide a simple description of such schedules.

In any optimal solution, the reading head will move to the leftmost request, then to the rightmost still unread request. Before reaching the leftmost request, the head may move back and forth in possibly intricate patterns to read relevant files first. We say that the solution includes the *detour* (a, b) , with a and b being two requested files such that $a \leq b$, if the head goes directly to $r(b)$ then back to $\ell(a)$ after first attaining $\ell(a)$. As shown previously [6] and later stated formally in our setting (see Lemma 1), there always exists an optimal solution which can be described only via a set of detours. Furthermore, a detour can be totally surrounded by a later one (*i.e.*, (a_1, b_1) and (a_2, b_2) with $a_1 < a_2 < b_2 < b_1$) but otherwise two detours cannot intersect each other (*i.e.*, (a_1, b_1) and (a_2, b_2) with $a_1 \leq a_2 \leq b_1 \leq b_2$).

Figure 1 illustrates a possible solution while Figure 2 shows detours overlapping in a suboptimal manner.

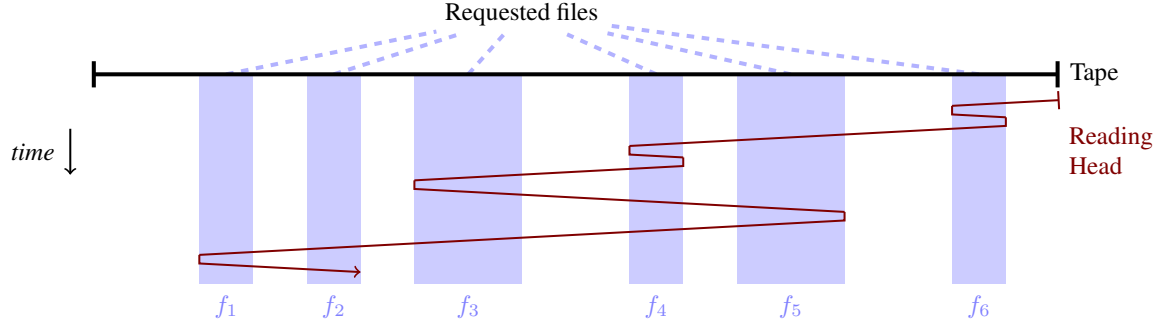


Figure 1: Example of schedule for reading six files described by the $[(f_6, f_6), (f_4, f_4), (f_3, f_5)]$ detour list. Note the delays caused by U-turn penalties.

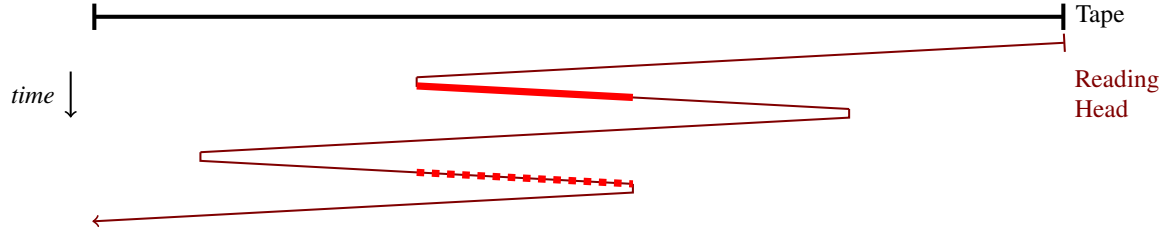


Figure 2: Example of non-optimal schedule. In the second detour, the movement in thick dotted lines is useless as these files have already been read earlier (thick solid line).

We denote this property on the set of detours in any optimal solution as being *strictly laminar*, following a definition of *laminar* used in the scheduling literature, see for instance [9]. We consider that all solutions contain the detour (f_{n_1}, f_{n_f}) , which reads all skipped files, even if the last movements may not count towards the objective as the rightmost requests may have already been served.

An unread file at the right of the current reading head position is called *skipped*. It will be read later when the head moves back to the right, possibly after the head read the leftmost file. For instance, on Figure 1, when f_4 is first reached by the head, f_5 is skipped, but when the head first reaches f_2 , no file is skipped.

4.2 Existing algorithms

One of the simplest algorithm would be to make no detour. The head simply moves to the leftmost requested file and then reads all files left-to-right. Despite minimizing the makespan, it can be arbitrarily far from the optimal solution in our model [6]. We refer to this algorithm as **NODETOUR**.

The opposite strategy would be to perform a detour on each requested file. This algorithm, named **GS** for Greedy Scheduling, has been proved to be a 3-approximation without U-turn penalties [6]. But of course harsh penalties can arbitrarily degrade its guarantees.

To improve the basic solution offered by **GS**, detrimental detours can be detected in multiple evaluation passes and filtered out in the **FSG** algorithm [7].

As **FSG** does not benefit from multi-file detours, the same authors designed the **NFGS** algorithm. In essence, for each pair of files $a < b$ starting from the left, it is tested whether it would be beneficial to add the detour (a, b) , after removing the detour starting from a if it existed. Despite its relatively large time complexity, **NFGS** remains very greedy in nature, definitely sealing any detour that seemed beneficial. A variant exploring only detours spanning over $O(\log n_{req})$ requested files, **LOGNFGS**, has been proposed to trade search space for running time.

Note that the algorithms **FGS**, **NFGS**, and **LOGNFGS** can be adapted to take into account the U-turn penalty in their decisions, although losing their approximation factor of 3 which was inherited from **GS**. We provide a description in Appendix A for completeness.

The structure of existing solutions, relying on greedy evaluation passes, illustrates the difficulty of the problem. The decision of making a detour or not depends on what happens before (a detour increases the delay on skipped files) and after (subsequent detours will increase the delay on files that have been skipped). Detours can also be intricate, as shown by Figure 1. Thus it seems hardly possible to take correct decisions on detours when each decision may influence the others. Consequently, Cardonha and Real [7] only considered a very restricted model (identical file sizes and a single request per file) in which the exact solution is simple but did not otherwise get any algorithm with an approximation ratio below 3.

4.3 Algorithm

Here, we describe the **DP** dynamic programming algorithm. It uses carefully selected memoization to store the cost of specific solutions used to build an optimal schedule.

The dynamic program cells have a number and three parameters: two requested files a and b and a number $n_{skip} < n$. The objective for each cell is to compute the best possible strategy for the reading head between $r(b)$ and $\ell(a)$ knowing that:

1. there is a detour (a, f) for some file $f \geq b$,
2. there is no detour (f_1, f_2) for any files f_1, f_2 satisfying $a < f_1 < b < f_2$,
3. when the reading head reaches $r(b)$, exactly n_{skip} files have been skipped.

The content of the cell describes the impact on the total cost of the movement made by the reading head between the first time it reaches $r(b)$ and the first time it reaches $r(b)$ after having read a . In other words, it equals the sum of the lengths for all requests on any file f of the “unnecessary” paths traversed by the head in this time interval and before serving the file f . Unnecessary means that we do not count the cost that would also be incurred to *VirtualLB* on a file f between a and b , as it is inevitable and this simplifies the formulas. The U-turn penalty on a is therefore not counted as *VirtualLB* would also have one U-turn penalty, but other U-turn penalties in this interval are counted.

We define $n_\ell(b)$ as the number of requests on files located on the left of b , excluding b , and let $left(b)$ be the closest requested file located to the left of b .

The value of cell $T[a, b, n_{skip}]$ is then defined as follows:

- If $b = a$, then there is a detour from $\ell(b)$ to at least $r(b)$ so we delay all pending requests by $2s(b)$, and incur no additional cost to b , see Figures 3 and 4. Therefore,

$$T[b, b, n_{skip}] = 2 \cdot s(b) \cdot (n_{skip} + n_\ell(b)).$$

- Otherwise, let $F_{a,b}$ be the set of requested files located between a and b excluding a . There are several possibilities to consider to determine the value of the cell: either b is skipped (it will be read with the detour starting from a), or read sooner than by the detour starting from a . In the latter case, it is read on a detour ending on b as there is no detour going to the right of b starting righter than a . This detour can start from any file in $F_{a,b}$. Then, we have:

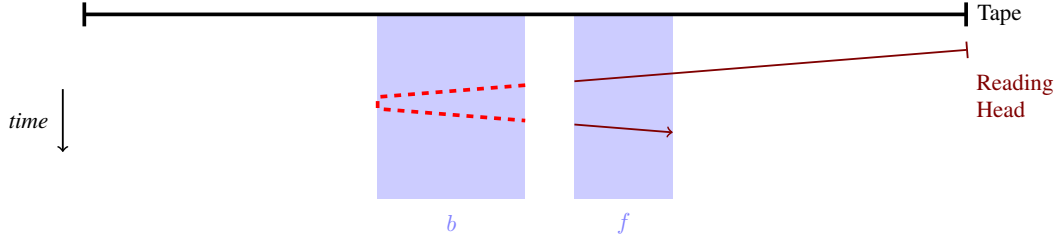


Figure 3: Cost incurred by a detour over file b to a skipped file f . The solid line represents the shortest path to serve f . The red dotted line represents the delay incurred by this detour to the service time of f . Other detours are not illustrated here. Subsequent figures follow the same logic.

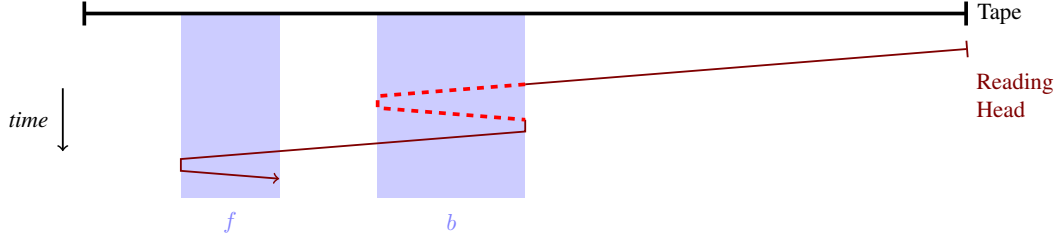


Figure 4: Cost incurred by the detour over b to a left file f .

$$\begin{aligned} skip(a, b, n_{skip}) &:= T[a, left(b), n_{skip} + x(b)] \\ &\quad + 2 \cdot (r(b) - r(left(b))) \cdot (n_{skip} + n_\ell(a)) \\ &\quad + 2 \cdot (\ell(b) - r(left(b))) \cdot x(b) \end{aligned}$$

$$\begin{aligned} detour_c(a, b, n_{skip}) &:= T[a, left(c), n_{skip}] + T[c, b, n_{skip}] \\ &\quad + 2 \cdot (r(b) - r(left(c))) \cdot (n_{skip} + n_\ell(a)) \\ &\quad + 2 \cdot U \cdot (n_{skip} + n_\ell(c)) \end{aligned}$$

$$T[a, b, n_{skip}] = \min \left(skip(a, b, n_{skip}) ; \min_{c \in F_{a,b}} detour_c(a, b, n_{skip}) \right)$$

In the first case, we recurse on a smaller window skipping file b , hence increasing n_{skip} . We also account for the cost of the detour starting from a over the files between $left(b)$ and b for the requests that will be fulfilled later. The differences with earlier are that (1) we also have to account for the cost to traverse the unrequested files at the left of b and (2) requests between a and $left(b)$ are served before the head comes back to the right, hence there are $n_\ell(a)$ delayed files and not $n_\ell(b)$. See Figures 5 and 6.

Finally, we account for the additional cost to serve b not covered by the recursive call: the path over the unrequested files directly at the left of b , see Figure 7.

In the second case, we have a detour (c, b) for some c in $F_{a,b}$. Hence, all these files will be read when the head reaches $left(c)$ so we do not change n_{skip} in the recursive calls. We still need to account for the cost of the detour starting from a over the interval $(r(left(c)), b)$. See Figures 8 and 9. We also charge here the U-turn penalties for all requests who will be served after the head reaches a , i.e., for all pending

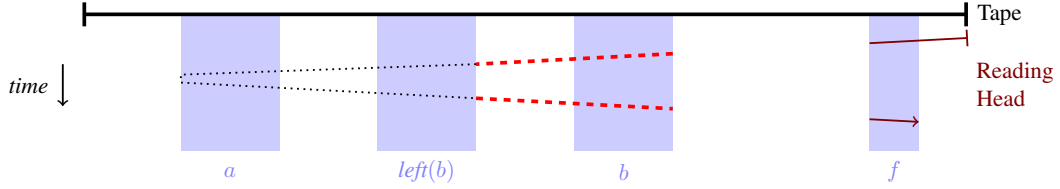


Figure 5: Impact of $skip(a, b, n_{skip})$ on a skipped file f . The thin dotted line represents the recursively computed impact (which may include subsequent detours), and the dashed line the impact directly accounted for.

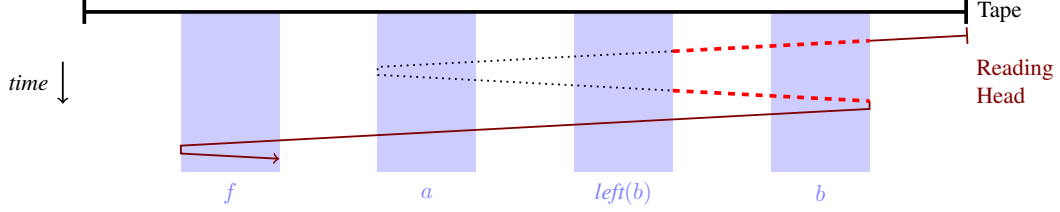


Figure 6: Illustration of the impact of $skip(a, b, n_{skip})$ on a left file f .

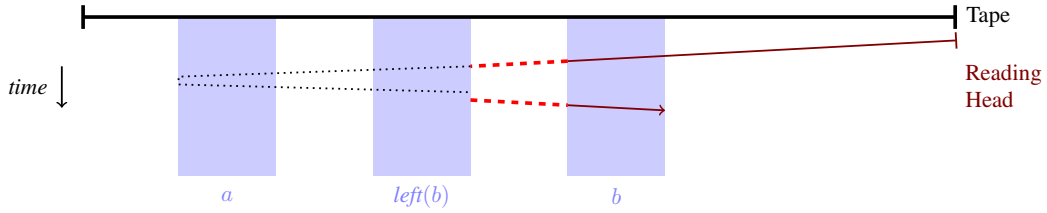


Figure 7: Impact of $skip(a, b, n_{skip})$ on b .

requests for which the U-turn at c is not the last one before they get served (the second U-turn penalty charged is for the U-turn occurring at b after the detour (c, b)).

Then, the overall solution can be computed through the call to $T[f_1, f_{n_f}, 0]$. The structure of the recursive calls minimizing this value leads to the detours taken by the underlying optimal solution.

4.4 Proof of the algorithm

First, we need a structural result to guarantee that the restriction to strictly laminar detours preserves the optimal solution. A similar result has been established in [6]. We state it here for self-consistency and a more precise result.

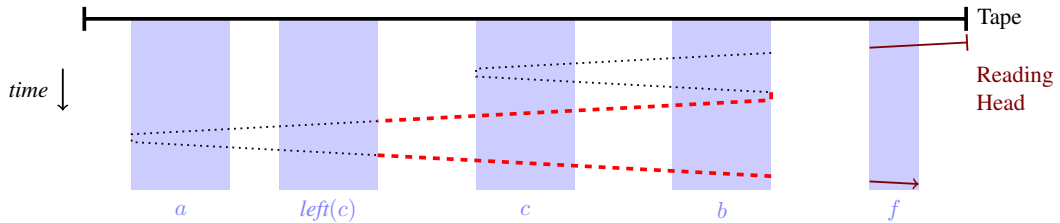


Figure 8: Impact of $detour_c(a, b, n_{skip})$ on a skipped file f .

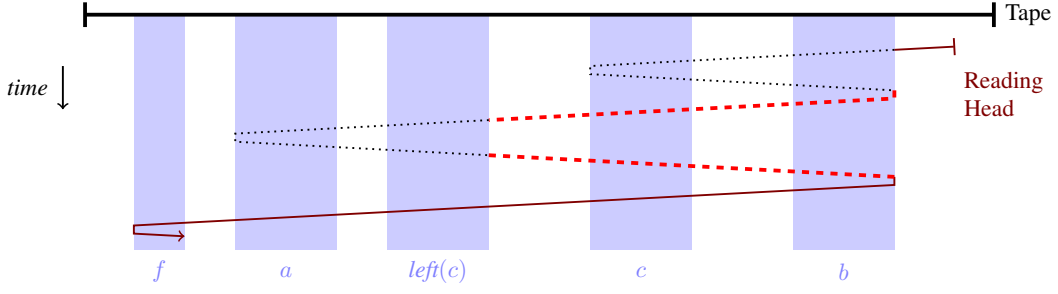


Figure 9: Impact of $\text{detour}_c(a, b, n_{\text{skip}})$ on a left file f .

Lemma 1. *There exists an optimal solution composed only of strictly laminar detours.*

Proof. Consider an optimal solution. Once the leftmost file is reached, it must go straight to the rightmost unread file. We now consider the part of solution before the leftmost file is reached.

Each time the head turns to the right at position x , it has to turn back to the left later at point y . It cannot turn again to the right before reaching x as this is suboptimal: no new file between x and y can be read this way. Furthermore, x must be the left of a requested file a and y the right of a requested file b or this is suboptimal. So the solution made a detour (a, b) . Continuing this analysis, we can decompose the optimal solution as a set of detours, counting again a global detour (f_1, f_{n_f}) . Note that we have shown that all detours start and end at the same position x , so detours are done in a non-increasing order of the left file.

We now show that these detours are strictly laminar. Assume there are two detours (a_1, b_1) and (a_2, b_2) with $a_1 \leq a_2 \leq b_1 \leq b_2$. After the first detour (a_2, b_2) is done, all files between a_2 and b_2 , so between a_2 and b_1 are read. So the second detour (a_1, b_1) can be shortened to $(a_1, \text{left}(a_2))$ if $a_1 < a_2$ or removed if $a_1 = a_2$: no file is read later and the cost does not increase for any file.

This concludes the lemma. \square

We are now ready to prove the correctness of **DP**. This proof relies on an induction involving several case distinctions ensuring every cost is counted once. It requires some technical care to precisely define which cost is counted at each step.

Theorem 1. **DP** solves optimally LTSP in time $O(n_{\text{req}}^3 \cdot n)$.

Proof sketch. The complexity follows from the dynamic programming definition: there are $O(n_{\text{req}}^2 \cdot n)$ cells which are each computed in time $O(n_{\text{req}})$.

We show for all a, b, n_{skip} by induction on $b - a$ that the computation of cell $T[a, b, n_{\text{skip}}]$ is correct. Specifically, our induction hypothesis considers any best solution $S_{a, b, n_{\text{skip}}}$ of the problem given three additional constraints: (1) there is a detour starting from a and going to b or a righter file; (2) there is no detour starting between $r(a)$ and $\ell(b)$ and going to a file righter than b ; and (3) when the reading head first reaches $r(b)$, exactly n_{skip} files have been skipped. Let t_1 be the time when the reading head first reaches $r(b)$ and t_2 be the first time the reading head reaches $r(b)$ (before performing a potential U-turn) after having read a in $S_{a, b, n_{\text{skip}}}$. For each file f , let $t(f)$ the time when it is served in $S_{a, b, n_{\text{skip}}}$. For each file $f \leq b$, let $\text{VirtOPT}_b(f) = r(b) - \ell(f) + s(f) + U$ be the minimum cost to serve f by a virtual head starting at $r(b)$ and $\text{VirtOPT}_b(f) = 0$ for $b > f$. See Figure 10.

The hypothesis is that cell $T[a, b, n_{\text{skip}}]$ is equal to the sum for all files f of the impact $\text{Delay}_{t_1, t_2}(f)$ of what happens between t_1 and t_2 in $S_{a, b, n_{\text{skip}}}$ on the service time of f , with a basis corresponding to VirtualLB , i.e.,

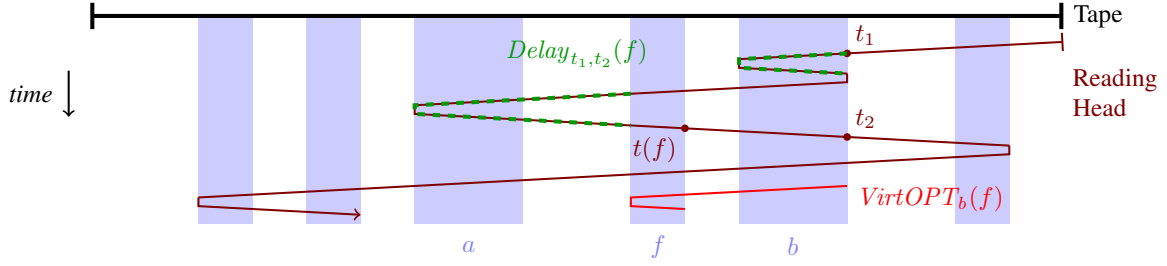


Figure 10: Illustration of t_1 , t_2 , $t(f)$, $VirtOPT_b(f)$ and $Delay_{t_1,t_2}(f)$ for $f \leq b$.

$$T[a, b, n_{skip}] = \sum_f x(f) \cdot Delay_{t_1,t_2}(f) \quad (1)$$

$$\begin{aligned} \text{with : } Delay_{t_1,t_2}(f) &:= 0 && \text{if } t(f) \leq t_1 \\ Delay_{t_1,t_2}(f) &:= t_2 - t_1 - U && \text{if } t(f) > t_2 \\ Delay_{t_1,t_2}(f) &:= t(f) - t_1 - VirtOPT_b(f) && \text{if } t_1 < t(f) \leq t_2. \end{aligned}$$

Intuitively, for files served after t_2 , the reading head comes back at the place it had in t_1 at time t_2 , with the opposite orientation. The delay is however not equal to $t_2 - t_1$ because we should not count the U-turn penalty here if a skipped file on the right of b is read within the same detour starting on a . Therefore, the delay equals $t_2 - t_1 - U$. Counting the cost based on *VirtualLB* allowed to simplify the computations in several places, but in this definition it leads to a less intuitive value of the delay. For files served between t_1 and t_2 , the file is served at $t(f)$ and we subtract $VirtOPT_b(f)$ to obtain the additional cost on top of the virtual lower bound.

We now show by induction on $b - a$ that Equation (1) is correct. First, consider $T[b, b, n_{skip}]$ for any b, n_{skip} . There are four types of files to consider.

- $f = b$: we have $t(f) = t_1 + 2s(b) + U$ and $VirtOPT_b(f) = 2s(b) + U$ so $Delay_{t_1,t_2}(f) = 0$,
- $f > b$ and is not skipped: we have $t(f) \leq t_1$ so $Delay_{t_1,t_2}(f) = 0$,
- $f > b$ and is skipped: we have $t(f) > t_2$ so $Delay_{t_1,t_2}(f) = 2s(b) + U - U$,
- $f < b$: we have $t(f) > t_2$ so $Delay_{t_1,t_2}(f) = 2s(b)$.

Overall, there are $n_{skip} + n_\ell(b)$ files who have a delay equal to $2s(b)$ so:

$$\sum_f x(f) \cdot Delay_{t_1,t_2}(f) = 2 \cdot s(b) \cdot (n_{skip} + n_\ell(b)) = T[b, b, n_{skip}].$$

This completes the base case of the induction ($b - a = 0$).

Now, consider $T[a, b, n_{skip}]$ for any values of a, b and n_{skip} such that $a < b$ and assume the induction hypothesis. We want to show that:

$$T[a, b, n_{skip}] = \sum_f x(f) \cdot Delay_{t_1,t_2}(f). \quad (2)$$

We consider two cases on the structure of $S_{a,b,n_{skip}}$: either b is served after a or before a . Assume first b is served after a . We want to show that in this case, we have:

$$\begin{aligned}
\sum_f x(f) \cdot \text{Delay}_{t_1, t_2}(f) &= \text{skip}(a, b, n_{\text{skip}}) \\
&= T[a, \text{left}(b), n_{\text{skip}} + x(b)] + 2 \cdot (r(b) - r(\text{left}(b))) \cdot (n_{\text{skip}} + n_\ell(a)) \\
&\quad + 2 \cdot (\ell(b) - r(\text{left}(b))) \cdot x(b).
\end{aligned} \tag{3}$$

Let t'_1 (resp. t'_2) be the first time when the reading head reaches $r(\text{left}(b))$ (resp. reaches $r(\text{left}(b))$) after having read a). See Figure 11. So $t'_1 = t_1 + r(b) - r(\text{left}(b))$ and $t'_2 = t_2 - r(b) + r(\text{left}(b))$. By the induction hypothesis, as (1) there is a detour from a to a file righter than $\text{left}(b)$ (2) there is no detour starting between $r(a)$ and $\ell(\text{left}(b))$ and going to a file righter than $\text{left}(b)$ (because of the definition of $S_{a, b, n_{\text{skip}}}$ and the assumption that b is served after a) and (3) exactly $n_{\text{skip}} + x(b)$ files are skipped at time t'_1 , we have by the induction hypothesis:

$$T[a, \text{left}(b), n_{\text{skip}} + x(b)] = \sum_f x(f) \cdot \text{Delay}_{t'_1, t'_2}(f).$$

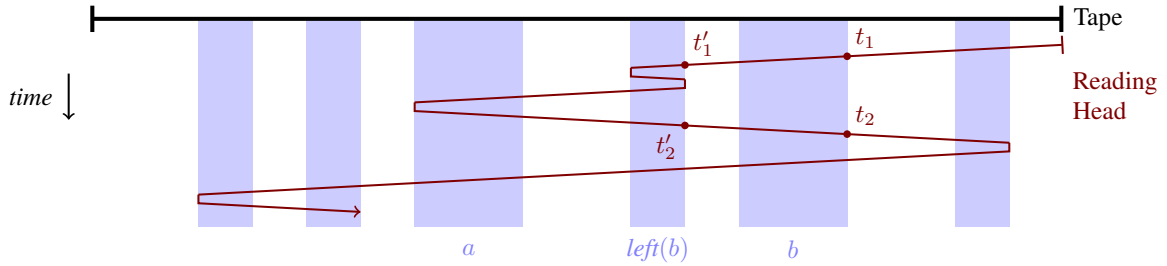


Figure 11: Illustration of t'_1 and t'_2 when b is skipped. The detour on $\text{left}(b)$ is not required but clarifies the definition of t'_2 .

We again consider several types of files f to determine $\text{Delay}_{t_1, t_2}(f)$ in function of $\text{Delay}_{t'_1, t'_2}(f)$.

- $f = b$: we have $t(f) = t'_2 + r(b) - r(\text{left}(b)) + U$ and $\text{VirtOPT}_b(f) = 2s(b) + U$ so we have

$$\begin{aligned}
\text{Delay}_{t_1, t_2}(f) &= t(f) - t_1 - \text{VirtOPT}_b(f) \\
&= t'_2 + r(b) - r(\text{left}(b)) + U - (t'_1 - (r(b) - r(\text{left}(b)))) - 2s(b) - U \\
&= t'_2 - t'_1 + 2 \cdot (r(b) - r(\text{left}(b))) - s(b) \\
&= \text{Delay}_{t'_1, t'_2}(f) + 2 \cdot (\ell(b) - r(\text{left}(b))).
\end{aligned}$$

- $f > b$ and is not skipped: $t(f) < t_1$ so $\text{Delay}_{t_1, t_2}(f) = \text{Delay}_{t'_1, t'_2}(f) = 0$.
- $f > b$ and is skipped: we have $\text{Delay}_{t_1, t_2}(f) = t_2 - t_1 - U = \text{Delay}_{t'_1, t'_2}(f) + 2 \cdot (r(b) - r(\text{left}(b)))$.
- $f < a$: same as the previous case.
- $a \leq f \leq \text{left}(b)$: we have $\text{VirtOPT}_b(f) = \text{VirtOPT}_{\text{left}(b)}(f) + r(b) - r(\text{left}(b))$ so

$$\begin{aligned}
\text{Delay}_{t_1, t_2}(f) &= t(f) - t_1 - \text{VirtOPT}_b(f) \\
&= t(f) - t_1 - \text{VirtOPT}_b(f) + \text{Delay}_{t'_1, t'_2}(f) - (t(f) - t'_1 - \text{VirtOPT}_{\text{left}(b)}(f)) \\
&= \text{Delay}_{t'_1, t'_2}(f) + (t'_1 - t_1) - (r(b) - r(\text{left}(b))) \\
&= \text{Delay}_{t'_1, t'_2}(f).
\end{aligned}$$

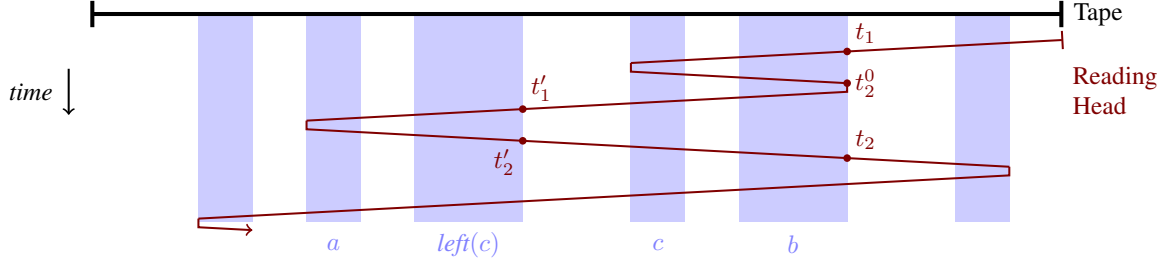


Figure 12: Illustration of t_2^0 , t'_1 and t'_2 when b is not skipped.

Therefore, we obtain Equation (3).

Now, assume b is served before a . This means that there is a detour from some file $c > a$ to a file at least as right as b . Furthermore, as we assumed that $S_{a,b,n_{skip}}$ has no detour from such a file c to a file righter than b , this means that there is a detour (c, b) . Therefore, by the laminar property of Lemma 1, and the optimality of $S_{a,b,n_{skip}}$, there is no detour from a file lefter than c to a file in $[c, b]$. We want to show that in this case, we have:

$$\begin{aligned} \sum_f x(f) \cdot \text{Delay}_{t_1, t_2}(f) &= \text{detour}_c(a, b, n_{skip}) \\ &= T[a, \text{left}(c), n_{skip}] + T[c, b, n_{skip}] \\ &\quad + 2 \cdot (r(b) - r(\text{left}(c))) \cdot (n_{skip} + n_\ell(a)) \\ &\quad + 2 \cdot U \cdot (n_{skip} + n_\ell(c)). \end{aligned} \quad (4)$$

First we argue that $S_{a,b,n_{skip}}$ is a solution compatible with the two cells queried in the expression above. Regarding $T[a, \text{left}(c), n_{skip}]$, we have:

1. a detour from a to a file righter than $\text{left}(c)$,
2. no detour from a file in $[a, \text{left}(c)]$ to a file righter than $\text{left}(c)$ as there is none righter than b by definition of $S_{a,b,n_{skip}}$ and there is none between c and b because detours are laminar and there is a detour (c, b) ,
3. exactly n_{skip} files have been skipped when reaching $r(\text{left}(c))$ as all files between c and b are read during the detour (c, b) .

Similarly, regarding $T[c, b, n_{skip}]$, we have (1) a detour (c, b) by assumption, (2) no detour from a file in $[c, b]$ to a file righter than b by definition of $S_{a,b,n_{skip}}$, and (3) exactly n_{skip} files skipped.

We denote by t_2^0 the first time $r(b)$ is reached after having read c (before the U-turn penalty), $t'_1 = t_2^0 + U + r(b) - r(\text{left}(c))$ the first time $r(\text{left}(c))$ is reached and by $t'_2 = t_2 - r(b) + r(\text{left}(c))$ the first time $r(\text{left}(c))$ is reached after having read a . Note that $t_1 < t_2^0 < t'_1 < t'_2 < t_2$, see Figure 12. Therefore, we obtain by the induction hypothesis:

$$T[a, \text{left}(c), n_{skip}] = \sum_f x(f) \cdot \text{Delay}_{t'_1, t'_2}(f) \quad \text{and} \quad T[c, b, n_{skip}] = \sum_f x(f) \cdot \text{Delay}_{t_1, t_2^0}(f).$$

We again consider several types of files f to determine $\text{Delay}_{t_1, t_2}(f)$:

- $f > b$ and is not skipped: all delays equal zero as $t(f) < t_1$.
- $c \leq f \leq b$: we have $\text{Delay}_{t_1, t_2}(f) = t(f) - t_1 - \text{VirtOPT}_b(f) = \text{Delay}_{t_1, t_2^0}(f)$ as $t(f) \leq t_2^0$ and $\text{Delay}_{t'_1, t'_2}(f) = 0$ as $t(f) < t'_1$.

- $a \leq f \leq \text{left}(c)$: we have:

$$\begin{aligned}
\text{Delay}_{t_1, t_2}(f) &= t(f) - t_1 - \text{VirtOPT}_b(f) \\
&= t(f) - t'_1 + t'_1 - t_1 - \text{VirtOPT}_{\text{left}(c)}(f) - (r(b) - r(\text{left}(c))) + t_2^0 - t_2^0 - 2U + 2U \\
&= (t(f) - t'_1 - \text{VirtOPT}_{\text{left}(c)}(f)) + (t'_1 - t_2^0 - U) - (r(b) - r(\text{left}(c))) \\
&\quad + (t_2^0 - t_1 - U) + 2U \\
&= \text{Delay}_{t'_1, t_2}(f) + 0 + \text{Delay}_{t_1, t_2^0}(f) + 2U.
\end{aligned}$$

- $f < a$: we have:

$$\begin{aligned}
\text{Delay}_{t_1, t_2}(f) &= t_2 - t_1 - U + 2U - 2U + t'_2 - t'_2 + t'_1 - t'_1 + t_2^0 - t_2^0 \\
&= (t'_2 - t'_1 - U) + (t_2 - t'_2) + (t'_1 - t_2^0 - U) + (t_2^0 - t_1 - U) + 2U \\
&= \text{Delay}_{t'_1, t'_2}(f) + 2 \cdot (r(b) - r(\text{left}(c))) + \text{Delay}_{t_1, t_2^0}(f) + 2U.
\end{aligned}$$

- $f > b$ and is skipped: same as the previous case.

Therefore, we get Equation (4).

We now conclude the proof of the induction.

As $S_{a, b, n_{\text{skip}}}$ must either serve b before a or include a detour (c, b) as argued earlier, we have:

$$\text{cost}(S_{a, b, n_{\text{skip}}}) \geq \min(\text{skip}(a, b, n_{\text{skip}}); \min_{c \in F_{a, b}} \text{detour}_c(a, b, n_{\text{skip}})) = T[a, b, n_{\text{skip}}].$$

And we get the equality by optimality of $S_{a, b, n_{\text{skip}}}$.

Finally, we get by induction, for all a, b, n_{skip} and $S_{a, b, n_{\text{skip}}}$:

$$T[a, b, n_{\text{skip}}] := \sum_f x(f) \cdot \text{Delay}_{t_1, t_2}(f).$$

Note that $S_{f_1, f_{n_f}, 0}$ is equal to the optimal solution of the problem. So, denoting by t_0 the starting time of the solution and t_{\max} the time at which the reading head would reach back the right of the tape in $S_{f_1, f_{n_f}, 0}$ (it may stop earlier if the rightmost file is not skipped), we get that the content of the cell $T[f_1, f_{n_f}, 0]$ is equal to:

$$\begin{aligned}
T[f_1, f_{n_f}, 0] &= \sum_f x(f) \cdot \text{Delay}_{t_0, t_{\max}}(f) \\
&= \sum_f x(f) \cdot (t(f) - t_0 - \text{VirtOPT}_{f_{n_f}}(f)) \\
&= \text{cost}(S_{f_1, f_{n_f}, 0}) - \text{VirtualLB}.
\end{aligned}$$

Therefore, we obtain that the optimal cost is equal to $\text{OPT} = T[f_1, f_{n_f}, 0] + \text{VirtualLB}$, which completes the proof. \square

4.5 Efficient heuristic

The complexity of **DP** may be prohibitive for an input containing hundreds of requested files. We address this issue by providing a lighter algorithm named **LOGDP**. It is equal to **DP** except that when computing $\text{detour}_c(a, b, n_{\text{skip}})$, c is restricted to be at most $\lambda \cdot \log n_{\text{req}}$ requested files apart from b , for a constant parameter λ . This reduces both the table dimensions and complexity to query a single cell so leads to a time complexity of $O(n_{\text{req}} \cdot n \cdot \log^2 n_{\text{req}})$. Only detours of span at most $\lambda \cdot \log n_{\text{req}}$ are then considered, and the solution returned is optimal among this class of schedules. The parameter λ can be adjusted to trade accuracy for computing time. We note that as this solution is by definition at least as good as **GS**, it is also a 3-approximation if $U = 0$.

5 Performance evaluation

In this section, we evaluate the performance, as the sum of service times of its generated sequence of detours, of our exact algorithm, **DP**, and its suboptimal version **LOGDP** with a reduced complexity on a real-world dataset. We also compare the performance of **DP** and **LOGDP** to existing algorithms [7] (see Section 4.2). Aiming for reproducibility, the source code used in this section¹ and the dataset² are freely available online.

5.1 Evaluated algorithms

We consider two variants of **LOGDP** with different values of the λ parameter, 1 and 5, that we denoted by **LOGDP(1)** and **LOGDP(5)**. Then, we adapted the **FGS**, **NFGS**, and **LOGNFGS** algorithms from [7] to take U-turn penalties into account. We further modified **NFGS** on three points which we believe were intended by the original authors as otherwise **NFGS** may not be as good as **FGS**, a property which was claimed in the paper. Details concerning our implementation can be found in Appendix A and in the source code. All these algorithms were implemented in a single-thread Python program.

For each tape, each algorithm needs the following inputs:

- an ordered list of indices of the files requested on the tape
- the number of requests for each requested file
- the size of all files on the tape
- the cost of the U-turn penalty

The output of an algorithm is a list of detours where a detour is a couple (a, b) which means that the head goes to the left of file a then to the right of file $b \geq a$. A value of $a = 0$ corresponds to the leftmost requested file on the tape. Then, we compute the sum of service times for each file request following the sequence of detours given by each algorithm.

5.2 Inputs from production logs

The IN2P3 Computing Center, from which our dataset comes, uses tape storage for long-term projects in High Energy Physics and Astroparticles physics. Its tape library is currently composed of 48 TS1160 drives and can store up to 6,700 20TB IBM Jaguar E tapes.

The raw dataset covers two weeks of activity. It contains millions of lines of reading, writing, and update requests with their associated timestamp. We applied several filtering steps to obtain the inputs needed by the algorithms. We restricted to reading requests, and selected a set of 169 tapes of interest storing 3,387,669 files. Each tape is divided into segments whose size and number depend on the tape. In a segment, files and *aggregates* of files are described by several features such as a position and a size. An aggregate is a batch of related files that can be written sequentially. A segment contains an aggregate if there is more than one file referenced in this segment. Within an aggregate, the position of a file is described a couple (position, offset) where the position corresponds to the beginning of the aggregate, thus the beginning of a segment, and the offset is the relative position of the file within the aggregate. Note that an aggregate can span across several segments. We discarded such aggregates and their associated requests to focus on aggregates lying on a single segment. Reading files inside an aggregate is not straightforward and generates a non-negligible overhead as the head is required to go to the start of the aggregate before reading a file.

Finally, we decided to consider that requesting a file within an aggregate will be treated as a request to read the whole aggregate. While this simplifies log filtering process, this assumption also corresponds to a common optimization strategy. Read aggregates are stored on disks when a file it contains is read for the first time. Then, all the subsequent accesses to files in this aggregate will avoid the large delays induced by tapes and benefit

¹<https://figshare.com/s/80cee4b7497d004dbc70>

²<https://figshare.com/s/a77d6b2687ab69416557>

of the smaller latency of disks. Consequently, we replace all the file requests in a given aggregate by a single request for a file of the size of this aggregate. Then we associate to this file a number of requests equal to the number of requested files in that aggregate.

To summarize, the processed dataset corresponds to a total of 119,877 files stored on the 169 tapes. We provide more details and statistics on this dataset in Appendix B.2. To the best of our knowledge, this is the first time that a realistic dataset for magnetic tape storage is made publicly available. In the context of the evaluation of the considered algorithms, this dataset corresponds to 169 distinct instances of LTSP to solve.

5.3 Simulation results

The evaluations presented in this section have been performed on a single server with two Intel Xeon Gold 6130 CPUs with 16 cores each. To compare the performance of the different algorithms, we use the generic *performance profile* tool [12]. We compute the cost of each algorithm on each instance of the dataset, normalize it by the optimal (**DP**), and report an empirical cumulative distribution function. For a given algorithm and an overhead τ expressed in percentage, we compute the fraction of instances for which the algorithm has a cost at most $(1 + \tau) \cdot \text{cost}(\mathbf{DP})$, and plot these results. Therefore, the higher the curve, the better the method. For instance, for an overhead of $\tau = 10\%$, the performance profile shows how often the performance of a given algorithm lies within 10% of the optimal solution.

We evaluate the algorithms on each of the 169 instances for three different values of the U-turn penalty U : (i) no penalty (ii) a penalty equals to half of the average size of a segment in the 169 considered tapes, and (iii) a penalty equivalent to the average size of a segment. While we have not yet modeled seeking and reading speeds of the head, such penalties whose values are extracted from features of the input instances are useful to evaluate the impact of increasing U on the performance of the algorithms.

Algorithms Performance Figure 13 shows the performance profiles of the algorithms without U-turn penalty. As expected, **GS** and **NODETOUT** show poor performance, with an overhead of more than 10% for **NODETOUT** over 60% of the instances. The **FGS**, **NFGS**, and **LOGNFGS** heuristics exhibit very similar performance, with an overhead of less than 2.5% over 80% of the test cases. Both variants of **LOGDP** heuristic slightly outperform the other heuristics. As expected, the higher λ , the closer to optimal the solution is.

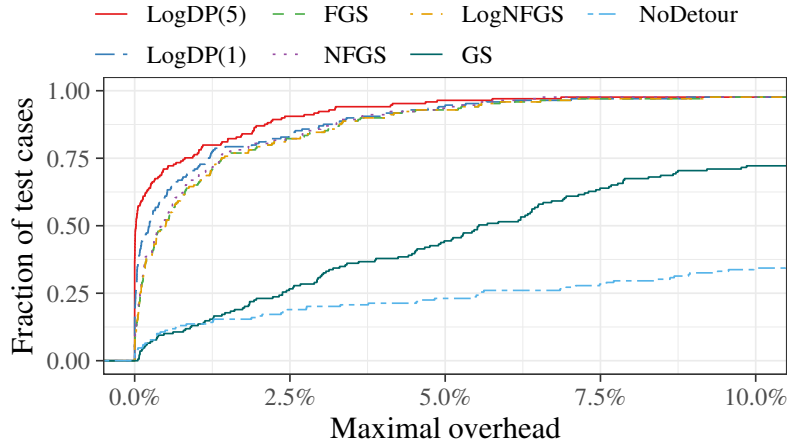


Figure 13: Performance of the different algorithms, when $U = 0$.

Figure 14 illustrates the algorithms performance with a U penalty equal to half of the average size of a segment. We see that the U-turn penalty increases the discrepancy between the performance of the **FGS**-like heuristics and **LOGDP**. Here, these heuristics cause at least 5% more overhead on almost all the instances than **LOGDP(1)**. It can even reach up to 10% more overhead than **LOGDP(5)**. The suboptimal solutions of

LOGDP variants are more robust to the increase of U , with an overhead of a few percent for **LOGDP(5)** when compared to **DP** for 75% of the inputs. The same trends can be observed in Figure 15, when the penalty is increased to the average size of a segment.

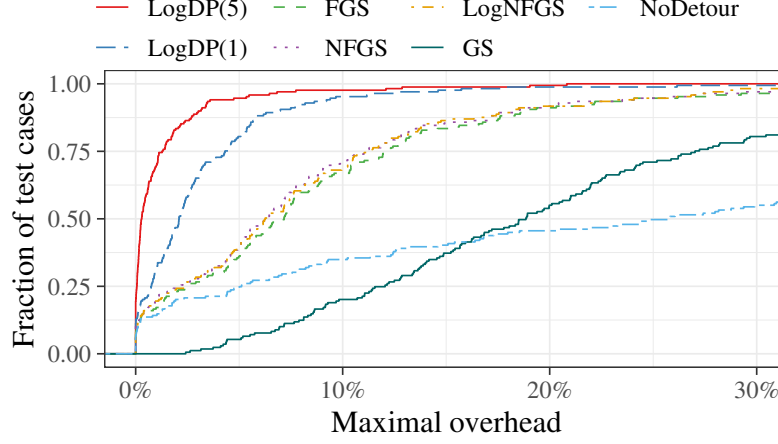


Figure 14: Performance of the different algorithms, when U is equal to half the average segment size.

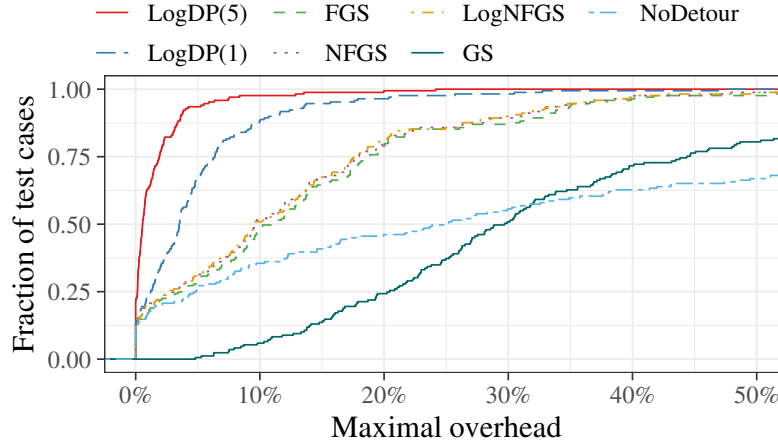


Figure 15: Performance of the different algorithms, when U is equal to the average segment size.

Time to solution The median running times for the algorithms **DP**, **LOGDP(5)**, **LOGDP(1)**, **NFGS** and **LOGNFGS** are around 281, 47, 5, 0.4 and 0.1 seconds respectively. The other algorithms have insignificant running times ($< 1\text{ms}$). The observed gains thus have to be nuanced by the required computing times of the algorithms. However, our single-thread Python implementation was not designed with performance in mind. The characteristics of the data set (a median $n > 2600$ much larger than $n_{req} < 150$) also explain the longer running times of **LOGDP** as the **FGS**-like algorithms complexity does not depend on n , see more details in Appendix B.2. The λ parameter can be used to obtain a faster version of **LOGDP** at the cost of lower performance. On large inputs (*i.e.*, list of requested files greater than 100), the cost of **DP** becomes prohibitive in a production context, making **LOGDP** variants good replacement candidates.

6 Conclusion

In this article we studied the Linear Tape Scheduling Problem, aiming at minimizing the average service time for read requests on a linear magnetic tape. We proposed an exact polynomial-time dynamic programming algorithm, solving this problem whose complexity was open until now. Then, we derived a low-cost suboptimal algorithm, whose performance outperforms existing heuristics on a realistic dataset extracted from the tape library logs of the IN2P3 Computing Center, a dataset we make publicly available.

This dataset could also be used for related problems such as k -server on the line for which few relevant datasets are available [17]. The remaining question on the theoretical side of LTSP resides in the possible improvements in the running time of an exact algorithm. The obvious generalization of the problem would be to consider the two-dimensional tape geometry, but we expect that such a model would quickly become intractable. We also discuss below how **DP** can be adapted to handle two minor extensions: arbitrary starting position of the head and a different reading speed.

Arbitrary starting position. The starting position of the reading head could be chosen at an arbitrary position X and the algorithm **DP** can be adapted to find the optimal solution: simply prevent any detour to start on the right of X . Indeed, this emulates a schedule in which the head initially moves from the rightmost file to X . No detour starting on the right of X would ever be needed later thanks to Lemma 1.

Different reading speed. We do not differentiate seeking speed, where the tape is required to move to a specific location, and reading speed, where data is actually output. The model could be tuned to accept such two different speeds, but we chose to keep it simpler by using a unique speed. This choice is motivated by the observation that reading times are much smaller than seeking times in the tapes operated in the studied computing center. **DP** could be easily transformed to account for such different speeds. The only limitation being that **DP** would require to read each file the first time it is traversed from left to right, which means that the solution returned would not be optimal on adversarial inputs requiring multiple back-and-forth seeks over a file before reading it.

Acknowledgments

We thank Pierre-Emmanuel Brinette for fruitful discussions. Experiments presented in this paper were carried out using the Grid'5000 testbed, supported by a scientific interest group hosted by Inria and including CNRS, RENATER and several Universities as well as other organizations (see <https://www.grid5000.fr>).

References

- [1] Foto Afrati, Stavros Cosmadakis, Christos H Papadimitriou, George Papageorgiou, and Nadia Pakostantinou. The Complexity of the Travelling Repairman Problem. *RAIRO-Theoretical Informatics and Applications-Informatique Théorique et Applications*, 20(1):79–87, 1986.
- [2] Mikhail J Atallah and S Rao Kosaraju. Efficient Solutions to Some Transportation Problems with Applications to Minimizing Robot Arm Travel. *SIAM Journal on Computing*, 17(5):849–869, 1988.
- [3] Antje Bjelde, Jan Hackfeld, Yann Disser, Christoph Hansknecht, Maarten Lipmann, Julie Meißner, Miriam Schlöter, Kevin Schewior, and Leen Stougie. Tight Bounds for Online TSP on the Line. *ACM Transactions on Algorithms*, 17(1):1–58, 2020.
- [4] Stefan Bock. Solving the Traveling Repairman Problem on a Line with General Processing Times and Deadlines. *European Journal of Operational Research*, 244(3):690–703, 2015. ISSN 0377-2217. doi: 10.1016/j.ejor.2015.02.009.

- [5] Eric Cano, Vladimír Bahyl, Cédric Caffy, Germán Cancio, Michael Davis, Oliver Keeble, Viktor Kotlyar, Julien Leduc, and Steven Murray. Cern tape archive: a distributed, reliable and scalable scheduling system. In *EPJ Web of Conferences*, volume 251, page 02037. EDP Sciences, 2021.
- [6] Carlos Cardonha and Lucas C Villa Real. Online Algorithms for the Linear Tape Scheduling Problem. In *Proceedings of the Twenty-Sixth International Conference on Automated Planning and Scheduling*, London, UK, June 2016.
- [7] Carlos Cardonha and Lucas Correia Villa Real. Theoretical and practical aspects of the linear tape scheduling problem. *CoRR*, abs/1810.09005v1, 2018. URL <http://arxiv.org/abs/1810.09005v1>.
- [8] K. Chaudhuri, B. Godfrey, S. Rao, and K. Talwar. Paths, trees, and minimum latency tours. In *44th Annual IEEE Symposium on Foundations of Computer Science, 2003. Proceedings.*, pages 36–45, 2003. doi: 10.1109/SFCS.2003.1238179.
- [9] Lin Chen, Nicole Megow, and Kevin Schewior. An $O(m)$ -Competitive Algorithm for Online Machine Minimization. *SIAM Journal on Computing*, 47(6):2057–2077, 2018.
- [10] Michael C Davis, Vladimír Bahyl, Germán Cancio, Eric Cano, Julien Leduc, and Steven Murray. CERN Tape Archive – from Development to Production Deployment. In *Proceedings of the 23rd International Conference on Computing in High Energy and Nuclear Physics*, volume 214 of *EPJ Web of Conferences*, page 04015. EDP Sciences, 2019. doi: 10.1051/epjconf/201921404015.
- [11] Willem E de Paepe, Jan Karel Lenstra, Jiri Sgall, René A Sitters, and Leen Stougie. Computer-Aided complexity Classification of Dial-a-Ride Problems. *INFORMS Journal on Computing*, 16(2):120–132, 2004.
- [12] D. Elizabeth Dolan and J. Jorge Moré. Benchmarking Optimization Software with Performance Profiles. *Mathematical Programming*, 91(2):201–213, 2002. doi: 10.1007/s101070100263.
- [13] Bruce K Hillyer and Avi Silberschatz. On the Modeling and Performance Characteristics of a Serpentine Tape Drive. *ACM SIGMETRICS Performance Evaluation Review*, 24(1):170–179, 1996.
- [14] IBM. *IBM System Storage Tape Drive 3592 SCSI Reference*. IBM, 2019.
- [15] Anna R Karlin, Nathan Klein, and Shayan Oveis Gharan. A (slightly) improved approximation algorithm for metric tsp. In *Proceedings of the 53rd Annual ACM SIGACT Symposium on Theory of Computing*, pages 32–45, 2021.
- [16] E. L. Lawler, Jan Karel Lenstra, A. H. G. Rinnooy Kan, and D. B. Shmoys. The traveling salesman problem: a guided tour of combinatorial optimization. *Wiley-Interscience Series in Discrete Mathematics*, 1985.
- [17] Alexander Lindermayr, Nicole Megow, and Bertrand Simon. Double coverage with machine-learned advice. *arXiv preprint arXiv:2103.01640*, 2021.
- [18] German Cancio Melia. Lto experiences at cern. HEPIX Workshop, <https://indico.cern.ch/event/730908/contributions/3153156/>, 2018.
- [19] Sachin More and Alok Choudhary. Scheduling queries for tape-resident data. In *European Conference on Parallel Processing*, pages 1292–1301. Springer, 2000.
- [20] Markus Mäsker, Lars Nagel, Tim Süß, André Brinkmann, and Lennart Sorth. Simulation and Performance Analysis of the ECMWF Tape Library System. In *Proceedings of the International Conference for High Performance Computing, Networking, Storage and Analysis*, pages 252–263, Salt Lake city, UT, November 2016. doi: 10.1109/SC.2016.21.

- [21] David Reine and Mike Kahn. Continuing the Search for the Right Mix of Long-term Storage Infrastructure – a TCO Analysis of Disk and Tape Solutions. Technical Report TCG2015006, The Clipper Group, Inc., 2015. [Online, Dec. 2021] www.clipper.com/research/TCG2015006.pdf.
- [22] Olav Sandsta and Roger Midtstraum. Improving the Access Time Performance of Serpentine Tape Drive. In *Proceedings 15th International Conference on Data Engineering*, pages 542–551, Sydney, Australia, March 1999. IEEE.
- [23] Jonathan Schaeffer and Andrés Gómez Casanova. Treqs: The tape request scheduler. In *Journal of Physics: Conference Series*, volume 331, page 042040. IOP Publishing, 2011.
- [24] René Sitters. The Minimum Latency Problem is NP-hard for Weighted Trees. In *Proceedings of the 9th International Conference on Integer Programming and Combinatorial Optimization*, pages 230–239, Cambridge, MA, May 2002. Springer.
- [25] René Sitters. Polynomial Time Approximation Schemes for the Traveling Repairman and Other Minimum Latency Problems. *SIAM Journal on Computing*, 50(5):1580–1602, 2021.
- [26] Xianbo Zhang, David Du, Jim Hughes, Ravi Kavuri, and Sun StorageTek. Hptfs: A high performance tape file system. In *Proceedings of 14th NASA Goddard/23rd IEEE conference on Mass Storage System and Technologies*. Citeseer, 2006.

A Precise description of the algorithms adapted from [7]

Each algorithm considered in this section takes the following inputs:

- an ordered list \mathcal{F} of indices of the files requested on the tape,
- the number of requests \mathcal{R} for each requested file,
- the size of all files on the tape \mathcal{T} ,
- the cost of the U-turn penalty U .

The output of an algorithm is a list of detours where a detour is a couple (a, b) which means that the reading head goes to the left of file a then to the right of file $b \geq a$. A value of $a = 0$ corresponds to the leftmost requested file on the tape.

We adapted **FGS**, **NFGS** and **LOGNFGS** from [7] to take into account U-turn penalties. We also modified **NFGS** on three points which we believe were intended by the original authors as otherwise **NFGS** may not be as good as **FGS**, a property which was claimed in the paper.

The pseudo-code depicted in this section is rather high-level, referring to mathematical inequalities without expliciting how to maintain each term. We explain the time complexity of our implementation and the low-level details can be checked directly in the source code.

A.1 Restating structural results

Before describing the algorithms, we need some preliminary definitions and results, on which the algorithms rely.

We say that a file f belongs to list of detours \mathcal{L} if and only if it is part of a detour of \mathcal{L} :

$$f \in \mathcal{L} \Leftrightarrow \exists (a, b) \in \mathcal{L} \mid a \leq f \leq b.$$

We assume that the tape starts at a requested file on its left to simplify the formulas: the reading head will have to go to the position 0, so at a distance $\ell(f)$ from the left of any file f (this assumption allows to drop additive $-\ell(f_1)$ terms).

The first result will be used by the algorithm **FGS**.

Lemma 2. Let \mathcal{L} be a list of single-file detours (f_i, f_i) and f be a file such that $(f, f) \in \mathcal{L}$. Then, $\text{cost}(\mathcal{L} \setminus \{(f, f)\}) < \text{cost}(\mathcal{L})$ if and only if:

$$2 \cdot x(f) \cdot \left(\ell(f) + \sum_{g < f \mid g \in \mathcal{L}} (s(g) + U) \right) < 2 \cdot (s(f) + U) \cdot \left(\sum_{g < f} x(g) + \sum_{g > f \mid g \notin \mathcal{L}} x(g) \right). \quad (5)$$

Proof. This equation with $U = 0$ corresponds to Corollary 4 in [7].

The left-hand side equals the delay added to the service time of f : for each request of f , the reading head has to go the left of the tape ($2\ell(f)$) and through all the detours $(g, g) \in \mathcal{L}$ on the left of f , where each detour adds a delay of $2(s(g) + U)$.

The right-hand side corresponds to the delay added to all other files than f by performing a detour of duration $2(s(f) + U)$ to serve f . The impacted files are the ones at the left of f and the skipped files. \square

We now define the function Δ required by the algorithm **NFGS**.

Definition 1. Let \mathcal{L} be a list of detours and (a, b) be a detour such that no detour in \mathcal{L} starts on a . We define:

$$\begin{aligned} \Delta(\mathcal{L}, (a, b)) = & 2 \cdot (r(b) - \ell(a) + U) \cdot \left(\sum_{f < a} x(f) + \sum_{f > b \mid f \notin \mathcal{L}} x(f) \right) \\ & - 2 \sum_{f \in [a, b] \mid f \notin \mathcal{L}} x(f) \cdot \left(\ell(a) + \sum_{(f', g') \in \mathcal{L} \mid f' < a} (r(g') - \ell(f') + U) \right). \end{aligned}$$

This definition corresponds to Equation 4 in [7]. The idea, similarly to Equation (5), was to represent the difference between $\text{cost}(\mathcal{L} \cup \{(a, b)\})$ and $\text{cost}(\mathcal{L})$. We will show below that it actually only represent an upper bound on this difference. Assume first that (a, b) does not intersect with a detour of \mathcal{L} starting on the left of a . The first term corresponds to the right-hand-side of Equation (5) and equals the delay added to pending files when executing the detour (a, b) . The second term represents the reduction on the service time of the files in (a, b) which were skipped in \mathcal{L} : the time to go from $\ell(a)$ to the left of the tape and come back, including all subsequent detours. So, in this case, it indeed represents the difference intended.

The last sum of the definition of Δ was indexed by $f' < f$ instead of $f' < a$ in the last line of Equation 4 of [7], but not on the previous steps. Having an index $f' < f$ here would lead to an erroneously smaller value of Δ as every detour located between a and f would lead to a diminution of the value of Δ , while such detours impact the service time of f in the exact same way in both $\mathcal{L} \cup \{(a, b)\}$ and \mathcal{L} .

Now, assume there exists a detour (a_1, b_1) in \mathcal{L} such that $a_1 < a$ and $b < b_1$. Then we must have $\Delta \geq 0$ as no file f can be in $[a, b]$ but not in \mathcal{L} . Therefore, Δ does not model accurately this case, remark which contradicts the claim in [7] that $\Delta(\mathcal{L}, (a, b)) = \text{cost}(\mathcal{L} \cup \{(a, b)\}) - \text{cost}(\mathcal{L})$. This fact will require to correct the algorithm **NFGS**, as it relied on it to exhibit an approximation factor of 3.

A.2 Greedy Scheduling (GS)

The first algorithm proposed by [7] is named **GS** for greedy scheduling. It returns a list of all detours (f, f) such that f is a requested file. It is shown to be a 3-approximation when $U = 0$. Its time complexity is $O(n_{req})$.

A.3 Filtered Greedy Scheduling (FGS)

The next algorithm, **FGS**, is an improvement over **GS** by filtering out detrimental detours. Such detours are determined using Equation (5). As removing a detour may lead to another detour becoming detrimental, this subroutine is run n_{req} times, for a time complexity in $O(n_{req}^2)$ as the terms needed to evaluate Equation (5) can be maintained in constant time per iteration.

Algorithm 1: Greedy Scheduling (GS)

Input: $\mathcal{F}, \mathcal{R}, \mathcal{T}, U$ **Output:** A list of detours

```
1: Let  $res = \emptyset$ .
2: for  $f \in \mathcal{F}$  do
3:   Append  $(f, f)$  to  $res$ 
4: end for
5: return  $res$ 
```

Algorithm 2: Filtered Greedy Scheduling (FGS)

Input: $\mathcal{F}, \mathcal{R}, \mathcal{T}, U$ **Output:** A list of detours

```
1: Let  $res = \mathbf{GS}(\mathcal{F}, \mathcal{R}, \mathcal{T}, U)$ .
2: for  $_ \in \mathcal{F}$  do
3:   for  $(f, f) \in res$  do
4:     if Equation (5) is true then
5:       Remove  $(f, f)$  from  $res$ 
6:     end if
7:   end for
8: end for
9: return  $res$ 
```

A.4 Non-Atomic Filtered Greedy Scheduling (NFGS)

The next algorithm, **NFGS** [7], is an improvement over **FGS** by replacing some unique-file detours by more beneficial multi-files detours. Therefore, it is claimed to also offer an approximation ratio of 3 when $U = 0$ as its cost should be lower than **GS**.

On top of the small correction on Δ described before, we also modified the algorithm in Line 6 and added Lines 4, 7-9, and 12 in order to avoid cases in which the cost of **FGS** becomes larger than the one of **GS**.

First, Line 6, we replaced $\arg \min_{f' > f}$ by $\arg \min_{f' \geq f}$ as, otherwise, unique-file detours cannot be kept which increases the final cost compared to **GS**.

Then, the second issue is related to the false claim about Δ . As, when f is part of a detour started on the left, the value of Δ is never negative (and almost always positive), beneficial detours part of a longer detour cannot be kept by the original algorithm, which increases the final cost compared to **GS**. Therefore, the added lines recognize this case and never remove such a detour (f, f) by overwriting the value of f^* .

This algorithm has a time complexity of $O(n_{req}^3)$, dominated by the $O(n_{req}^2)$ evaluations of Δ which requires $O(n_{req})$ time to be computed.

A.5 Logarithmic Non-Atomic Filtered Greedy Scheduling (LOGNFGS)

The last algorithm we present in this document is a restriction of **NFGS** where the detour lengths are bounded by $\lambda \cdot \log n_{req}$ requested files. The original algorithm [7] was written with a value of $\lambda = 1$ but we add this parameter for a fair comparison with **LOGDP**. In the experiments, we use a parameter of 5 as our dataset presents values of n_{req} smaller than the dataset used in [7]. Its time complexity is $O(n_{req}^2 \log n_{req})$.

Algorithm 3: Non-atomic Filtered Greedy Scheduling (NFGS)

Input: $\mathcal{F}, \mathcal{R}, \mathcal{T}, U$ **Output:** A list of detours

```
1: Let  $res = \mathbf{FGS}(\mathcal{F}, \mathcal{R}, \mathcal{T}, U)$ .
2: Let  $RightestDetour = 0$ 
3: for  $f \in \mathcal{F}$  do
4:   Let  $WasADetour = True$  if  $(f, f) \in res$  else  $False$ 
5:   Let  $temp = res \setminus \{(f, f)\}$ 
6:   Let  $f^* = \arg \min_{f' \geq f} (\Delta(temp, (f, f')))$ 
7:   if  $\Delta(temp, (f, f^*)) \geq 0$  and  $WasADetour$  and  $RightestDetour > f$  then
8:      $f^* = f$ 
9:   end if
10:  if  $\Delta(temp, (f, f^*)) < 0$  then
11:    Add  $(f, f^*)$  to  $res$ 
12:     $RightestDetour = \max(RightestDetour, f^*)$ 
13:  end if
14: end for
15: return  $res$ 
```

Algorithm 4: Logarithmic Non-atomic Filtered Greedy Scheduling (LOGNFGS)

Input: $\mathcal{F}, \mathcal{R}, \mathcal{T}, U$ **Parameters:** λ **Output:** A list of detours

```
1: Let  $res = \mathbf{FGS}(\mathcal{F}, \mathcal{R}, \mathcal{T}, U)$ .
2: Let  $RightestDetour = 0$ 
3: for  $f \in \mathcal{F}$  do
4:   Let  $WasADetour = True$  if  $(f, f) \in res$  else  $False$ 
5:   Let  $temp = res \setminus \{(f, f)\}$ 
6:   Let  $f^* = \arg \min_{f' \geq f \text{ and } f' \leq f + \lambda \log n_{req}} (\Delta(temp, (f, f')))$ 
7:   if  $\Delta(temp, (f, f^*)) \geq 0$  and  $WasADetour$  and  $RightestDetour > f$  then
8:      $f^* = f$ 
9:   end if
10:  if  $\Delta(temp, (f, f^*)) < 0$  then
11:    Add  $(f, f^*)$  to  $res$ 
12:     $RightestDetour = \max(RightestDetour, f^*)$ 
13:  end if
14: end for
15: return  $res$ 
```

B Reproducibility artifact and dataset

This section is dedicated to the reproducibility of the performance evaluation results presented in Section 5. Section B.1 describes a dataset of reading requests on 169 tapes, associated to the description of all the files on these tapes. This dataset is available at <https://figshare.com/s/a77d6b2687ab69416557>. The data are extracted from real logs of a leading computing facility and is, to the best of our knowledge, the first one of its kind publicly available. Section B.2 contains all the necessary material to reproduce the simulation results presented in Section 5. This material is available in a reproducibility artifact freely accessible <https://figshare.com/s/80cee4b7497d004dbc70>. It contains all the instructions regarding the execution of the simulation code, the output data of the different experiments, and the scripts to generate the figures.

B.1 A public dataset of magnetic tape file description and reading requests

In this section, we introduce a dataset containing the position and size of files on magnetic tapes, associated to user reading requests on these tapes from a production system. The dataset is freely accessible online using the following link: <https://figshare.com/s/a77d6b2687ab69416557>.

Context

The IN2P3 Computing Center, from which our dataset is extracted, uses tape storage for long-term projects in the fields of Particle Physics and Astrophysics. In this context, we had access to logs of the tape system from a period of high activity. The center uses the Spectra Tfinity library, and has 48 reading engines TS1160 with 6700 Jaguar E magnetic tapes with a capacity of 20TB each.

The raw dataset covers three weeks of activities. It contains millions of lines of reading, writing and update requests with their associated timestamp. It also details positioning operations and delays of the device heads. For obvious privacy issues, we cannot make the whole raw dataset public, but only some anonymized features.

In this work, we were interested in getting a description of magnetic tapes (position and size of files on magnetic tapes), associated to user reading requests on these files. The former knowledge is accessed through description files of the tapes, given by the system. The latter is obtained from the raw logs, after several steps of filtering.

We first removed all lines from the raw dataset that do not concern reading operations. This gives us a list of 169 tapes, covering a total of 3,387,669 files. Each tape is divided into segments containing files or *aggregates* of files. The size and number of segments depend on the tape. In a segment, the files are described by several features such as position and size. The current setup in the computing center allows to write *aggregates* of files on the tapes, *i.e.*, a batch of related files that can be written sequentially. A segment contains an aggregate if there is more than one file referenced in this segment. Within an aggregate, the position of a file is given as a couple (position,offset) here the position is actually the beginning of the aggregate, thus the beginning of a segment. Note that an aggregate can span across several segments. We discarded such aggregates and their associated requests to focus on aggregates lying on a single segment. Reading files inside an aggregate is not straightforward and generates a non-negligible overhead as the head is required to go to the start of the aggregate before reading a file. To ease the extraction of our sequences of requests, we considered that a requested file inside an aggregate will be treated as a request to read the whole aggregate. Such a behavior actually represents a strategy of buffering when aggregates are stored on disks after a file is requested within, in order to avoid the costly operations of accessing a file in aggregates. Thus, all the file requests in the same aggregate are replaced by a single request for a file of the size of this aggregate, and we associate to this file a number of requests equal to the number of files in the aggregate.

Overall, the final processing of the logs gives us 169 tapes with a total of 119,708 files stored on it after the filtering of aggregates, according to the tape description files of the system at the considered period in the logs. The exploitation of the system logs allowed us to extract 28,853 unique file requests on these tapes, and a total of 615,324 user requests over these files.

This dataset is, to the best of our knowledge, the first publicly available dataset on magnetic tape storage. In the next paragraph, we describe the different files of the dataset.

Dataset content

Table 1 gives a brief summary of the dataset in terms of tape size and number of requests.

We now describe the content of the public folder.

We have a large panel of tape size, going to hundreds of files to thousands of files. The same observation stands for the number of file requests (31 to 852). Figure 16 represents the distribution of unique files requested for the different size of tapes. Even though we mostly have tapes of size less than a thousand files with a number of unique requested files less than 400, the dataset is not homogeneous and presents various amount of unique file requested on the tapes. We display in Figure 17, for each tape, the distribution of the total number of user requests with the number of unique files requested. We also observe that the total number of user requests is different between tapes having very similar number of unique files requested. Hence, we believe this dataset is heterogeneous and suitable for performance evaluation of a magnetic tape system storage.

‘list_of_tape.txt’ This file lists the name of the 169 tapes in the dataset. For each tape, there is a file listing all the user requests on this tape in the folder **requests**, and a file describing the content of the tape in the folder **tapes**. The tapes are named under the format *TAPEXXX.txt* where XXX varies from 001 to 169.

requests folder For each tape, this folder contains a request file with two columns *index*, *nb_requests*. The former refers to the index of the requested file on the tape (see **tapes** folder) associated to the number of requests for this file. The maximum number of distinct files requested for one tape is equal to 852, and the minimum number is 31. The median value is 148 requests (for a tape of size 531), and the mean is 170 requests. Regarding the total number of user requests on one tape, the maximum is 15477 and the minimum is 1182, for a median value of 2669 files and a mean of 3640.

tapes folder This folder contains a description file of each tape in the dataset. From the left (position 0) to the left of each tape, the file describes the different segments of the tape.

It contains four columns *id*, *cumulative_position*, *segment_size*, *index*. The *id* column corresponds to the id number of the segment on the tape given by the system. The next two columns respectively refer to the cumulative position of the segment from the left of the tape, and its size. Finally, the column *index* is used as the id of the file on the tape starting from 1 for the leftmost file. This fourth column is used to match the *index* column of the **requests** files. The largest tape contains 4141 files, and the smallest one 111. The median size is 489 files and the mean size is 708 files.

	Tape size (n_f)	# Files Requested (n_{req})	# Total User Requests (n)
Maximum	4141 (TAPE104.txt)	852 (TAPE109.txt)	15477 (TAPE139.txt)
Minimum	111 (TAPE010.txt)	31 (TAPE115.txt)	1182 (TAPE082.txt)
Median	489 (TAPE118.txt)	148 (TAPE041.txt)	2669 (TAPE078.txt)
Mean	708	170	3640

Table 1: Overview of some dataset features.

Perspectives

This dataset allowed us to evaluate several algorithms on realistic data extracted from the logs of a production computing center. We expect this dataset to be a first step in the achievement of large-scale datasets of such types. Logs from a large time period can be envisioned as an extension to this dataset.

In this work, we only considered reading requests from user in the framework of the Linear Tape Scheduling Problem. However, the raw logs contains much more information that one could expect to use. Knowledge about time processing of reading operations and positioning operations performed by the multiple device heads

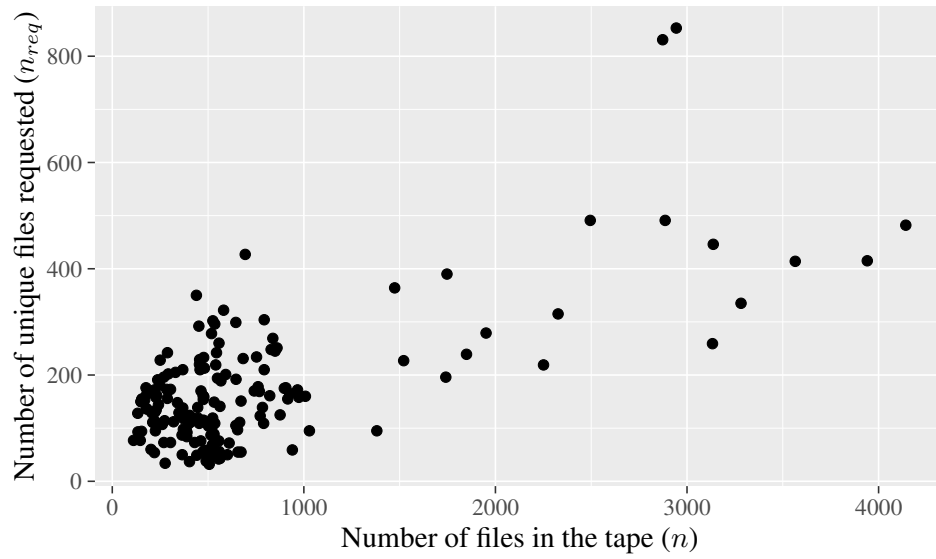


Figure 16: Illustration of the tape dataset with the number of files in each tape in function of the number of unique requested files in it.

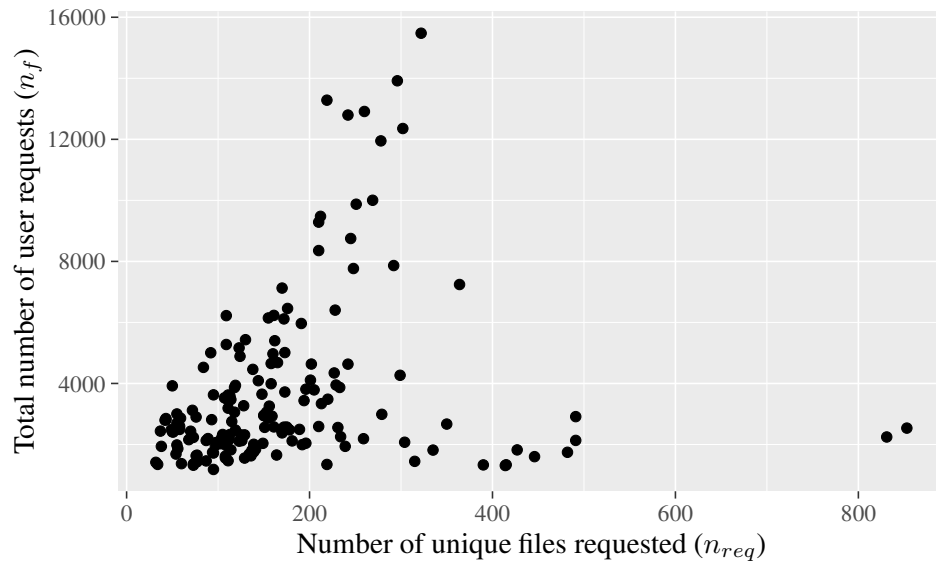


Figure 17: Illustration of the tape dataset with the number of unique requested files in each tape in function of the total number of user requests in it.

could be leveraged to better model seeking speed and reading speed. With a fast parsing of the logs, the positioning time seems to impact the performance much more than the reading time. Hence, modeling the seeking speed of the device seems to be important in order to provide realistic cost models of the process. Temporal aspects of the raw dataset could also be exploited for a usage in online problems, for instance.

B.2 Reproducibility artifact

This section provides all the details to reproduce the performance evaluation presented in Section 5. The complete artifact can be downloaded online: <https://figshare.com/s/80cee4b7497d004dbc70>.

‘input’ folder

This folder contains the data described in Section B.1. The reader is invited to refer to this section for comprehensive details about the dataset used for the performance evaluation, and how it has been generated. The folder ‘inputs’ contains the index of the files requested on a tape, associated to the number of requests on these files. The folder ‘tape’ describes the position and size of the files on a tape. Both folders are used as input of the algorithm (see **code** folder).

‘code’ folder

This folder contains a Python implementation of our algorithms, alongside the ones adapted from [7] used for baseline comparison. We carefully implemented the different strategies in a Python code, that are available in the *algorithms.py* file. The *main.py* file is dedicated to the execution of all algorithms on all the instances of the **input** folder. It directly parses the different files in the **input** folder to instantiate 4 different parameters of the algorithms:

- **files_requested**: the list of requested files on the tape, comes from the `index` column in the *input/requests/TAPEXXX.txt* files.
- **request_numbers**: the number of requests of each file in the above list. Extracted from the `nb_requests` column in the *input/requests/TAPEXXX.txt* files.
- **tape**: the list of all file sizes on the tape. Extracted from the `segment_size` column of the *input/tapes/TAPEXXX.txt* files/
- **right**: a list of the right ordinate of each file in **tape**. Obtained by computing the cumulative sum of tape

We also provide in the *draw.py* file a visualization tool of the device head trajectory depending on the list of detours given by the algorithms. This tool is automatically called in ‘main.py’ for each input and each algorithm.

To start the performance evaluation, one should just go into the **code** folder, and start the program using the **makefile**:

```
1 cd code ; make
```

It requires to have a python3 program on the machine. It can easily be installed on any Unix-like machine using the following command

```
1 sudo apt-get install python3
```

The performance evaluation in Section 5 uses Python3 version 3.9.2. The code has been executed on a cluster using two Intel Xeon Gold 6130 CPUs per node, with 16 cores each. The execution of the algorithms have been performed sequentially on a single core of a dedicated node to avoid external disturbances.

‘Run’ folder

This folder contains the performance of the different strategies evaluated in Section 5. For each algorithm, we recorded the cost induced by the list of detours in output and the simulation time to get the solution. We tested three different values of the U-turn penalty, that is a parameter:

- 0: no penalty
- 14254750000: it represents half of the average size of a tape segment according to our 169 input tapes.
- 28509500000: it represents the average size of a tape segment according to our 169 input tapes.

The file *results.csv* summarizes the cost of the list of detours induced by each algorithm, associated to the time-to-solution to get this list for each of the three penalties above presented. We also record the lower bound for each algorithm on each input.

‘Figure’ folder

This folder contains a R script to reproduce the figures presented in Section 5. This script processes the *run/results.csv* to output the performance evaluations that were reported.